Journal of Applied Electrochemistry **31**: 275–279, 2001.

Development and operation of a 150 W air-feed direct methanol fuel cell stack

D. BUTTIN[1]*, M. DUPONT[1], M. STRAUMANN[1], R. GILLE[1], J-C. DUBOIS[1], R. ORNELAS[2], G.P. FLEBA[2], E. RAMUNNI[3], V. ANTONUCCI[4], A.S. ARICÒ[4], P. CRETÌ[4], E. MODICA[4], M. PHAM-THI[5] and J-P. GANNE[5]
[1]*Sodeteg, 25, rue du Pont des Halles, Chevilly-Larue, 94666 Rungis Cedex, France*
[2]*De Nora Fuel Cells, Via Bistolfi 35, 20134 Milan, Italy*
[3]*De Nora, Via Bistolfi 35, 20134 Milan, Italy*
[4]*CNR–TAE Institute for Transformation and Storage of Energy, Salita S. Lucia sopra Contesse 39, 98126 S. Lucia, Messina, Italy*
[5]*Thomson–CSF/LCR, Domaine de Corbeville, 91404 Orsay, France*
*(*author for correspondence)*

Received 20 March 2000; accepted in revised form 28 July 2000

Key words: direct methanol fuel cells, fuel cell stack, fuel cell performance, Pt catalysts, Nafion 117®

Abstract

A five-cell 150 W air-feed direct methanol fuel cell (DMFC) stack was demonstrated. The DMFC cells employed Nafion 117® as a solid polymer electrolyte membrane and high surface area carbon supported Pt-Ru and Pt catalysts for methanol electrooxidation and oxygen reduction, respectively. Stainless steel-based stack housing and bipolar plates were utilized. Electrodes with a 225 cm^2 geometrical area were manufactured by a doctor-blade technique. An average power density of about 140 mW cm^{-2} was obtained at 110 °C in the presence of 1 M methanol and 3 atm air feed. A small area graphite single cell (5 cm^2) based on the same membrane electrode assembly (MEA) gave a power density of 180 mW cm^{-2} under similar operating conditions. This difference is ascribed to the larger internal resistance of the stack and to non-homogeneous reactant distribution. A small loss of performance was observed at high current densities after one month of discontinuous stack operation.

1. Introduction

In the last few decades, direct methanol fuel cells (DMFCs) have been actively investigated from both fundamental and applied points of view [1–26]. Many of the aspects related to the intrinsic mechanism of CH_3OH electrooxidation on Pt-based catalysts have been clarified and increasing efforts are currently being made on the development of small size DMFC prototypes. At present, the DMFC utilizes a polymer electrolyte membrane, such as Nafion®, on to which electrocatalyst-containing carbon cloth- or carbon paper-based electrodes are contacted on either side to form a membrane–electrode assembly (MEA). A carbon supported Pt–Ru alloy is frequently used as an electrocatalyst for methanol oxidation whereas oxygen reduction occurs at suitable rates on Pt catalysts [12–23]. The present Nafion® based perfluoro–sulfonic membranes are significantly permeable to methanol [14, 15]. The cross-over of CH_3OH molecules through the membrane leads to a parasitic methanol oxidation reaction at the Pt cathode surface that significantly lowers the cell potential [14]. Two strategies are currently being pursued to overcome this drawback, that is, oxygen-selective reduction catalysts and methanol resilient membranes [1, 8, 23]. Although a great deal of progress has been made, Nafion® membranes and Pt electrocatalysts still represent the most suitable choice for the production of experimental prototypes and for prolonged operation [5–10].

The DMFC devices have been characterized in terms of both performance and efficiency [22]. Recent results have shown interesting prospects for the application in the fields of electrotraction and portable power sources [7, 10, 22]. Yet, the demonstration of DMFC prototypes of suitable size has only recently been initiated [10]. The design and operation of these systems require the selection of proper components, cell housing and experimental conditions.

In this communication, the development of a 150 W air-feed direct methanol fuel cell stack within the framework of the NEMECEL project is described.

2. Experimental details

The DMFC stack was composed of five 225 cm^2 cells connected in series. The stack housing was developed and produced by De Nora Fuel Cells and Sodeteg. It was made up of stainless steel (AISI 316) end plates and

bipolar plates. No gold or other noble-metal plating was used. The materials were surface treated to avoid chemical and electrochemical corrosion. Both fuel and air were supplied from one side of the stack and distributed over the electrode backings through corrosion-resistant metallic foams. Reactant inlets/outlets were located in the same end plate. Each cell in the stack was intercalated with a cooling/heating section in which silicon oil or pressurized water was circulated through a thermostat in order to maintain the stack at the desired temperature. The cell temperature was measured through thermocouples located very close to each MEA. Both anodic and cathodic catalysts were synthesised at CNR–TAE Institute using a colloidal procedure. A continuous stirred tank reactor (CSTR) with a 12 litre reaction chamber was manufactured to produce the required amount of anodic and cathodic catalysts in one batch in order to have identical catalyst properties for each cell assembled in the stack. The anodic catalyst formulation was 85% Pt–Ru (1:1)/Vulcan XC. The methanol oxidation catalyst had an atomic Pt/Ru ratio of 1 and an average particle size of about 2 nm. The oxygen reduction catalyst was an 85% Pt/Vulcan with a mean particle size of 3.7 nm. The electrocatalytic activity of these materials was investigated in a 5 cm^2 single cell (GlobeTech) equipped with serpentine graphite flowfields before being used for large area MEA production. Electrodes with an area of 225 cm^2 and MEAs were fabricated at the Thomson–CSF/LCR Corporate Research Laboratory, using a procedure already developed at CNR–TAE [8, 12]. The electrodes consisted of carbon cloth, a diffusion layer (carbon cloth and Teflon®) and a reaction layer (catalyst and Nafion® ionomer). The Pt content was 2 mg Pt cm^{-2} on each electrode. Nafion 117® (DuPont) was selected as the membrane. The MEA was manufactured by hot pressing the components at 130 °C for 90 s. The stack test station was designed and manufactured by Sodeteg. A flow diagram of the DMFC stack plant is shown in Figure 1. All variables i.e. temperatures, pressures, reactant flows and electrochemical parameters such as stack current and voltage characteristics were computer-controlled and visualized. Indeed, a specific software program has been developed allowing direct piloting and continuous preview of the actuating gears on the interactive screen, recording and filing of all the data relating to a trial and management of all the safety thresholds for each critical parameter. Methanol and air were preheated at the desired temperature (110 °C methanol and 100 °C air) before being fed to the stack. 1 M aqueous methanol solution was supplied to the stack at a feed rate of 360 ml min^{-1}; air was humidified before being fed to the stack at 25 l min^{-1}. Most of the measurements were collected at 110 °C stack temperature; under such condition, a 1.5 atm backpressure was imposed in the anodic compartment, while the pressure in the cathodic compartment was 3 atm. Galvanostatic steady-state polarization curves were collected through an electronic load SDCH G4 300 2K 60 backed up with a power supply 7.5-250-3-D-10T-TC. Internal resistance was measured by the current-interruption method using a digital oscilloscope.

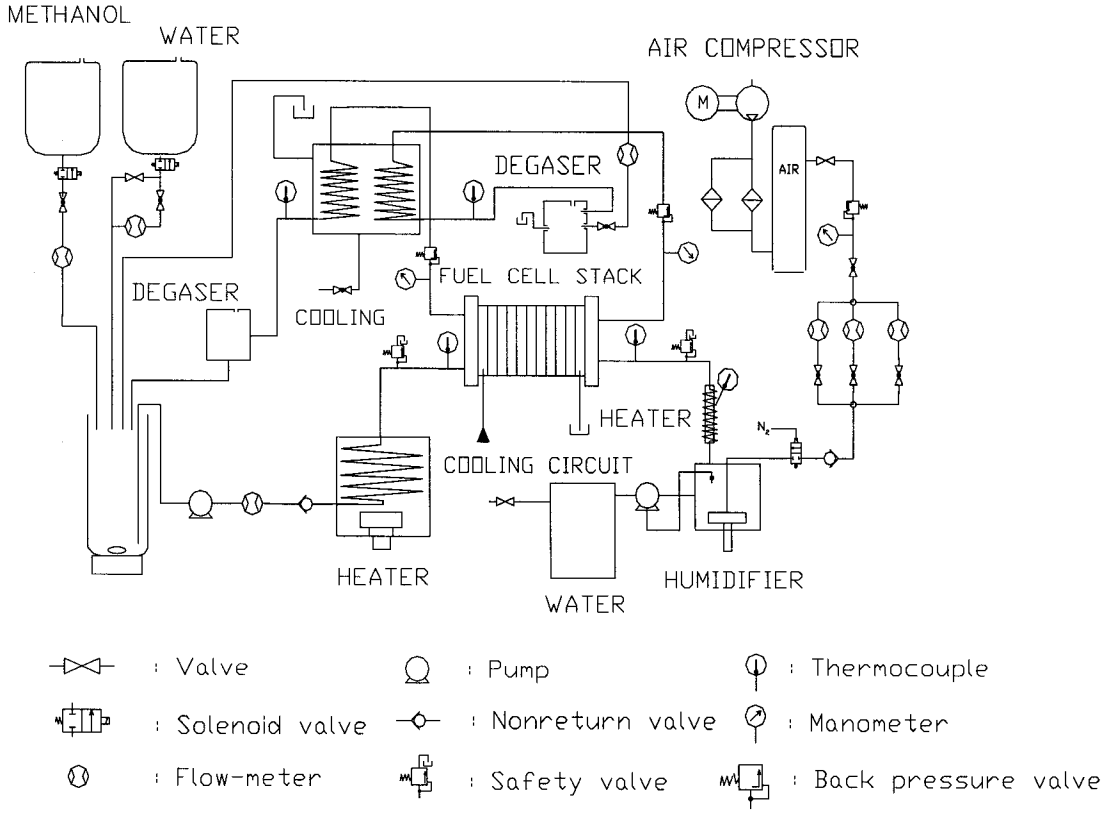

Fig. 1. Flow sheet of the DMFC stack plant.

3. Results and discussion

Galvanostatic steady-state polarization data for the five-cell air-feed stack at 110 °C are shown in Figure 2. The open circuit voltage approaches 4 V, yet a significant voltage loss (about 1 V) is observed at very low current densities indicating strong activation control. Almost linear behaviour is observed in the stack polarization curve up to 350 mA cm^{-2}. This reflects the presence of ohmic control. The curve slope is close to the value of the stack internal resistance determined by the current-interruption method (i.e., 5.5 mΩ). Accordingly, the average cell resistance is 0.25 Ω cm^2. Above 400 mA cm^{-2}, mass-transfer limitations play a significant role and the cell voltage drops significantly. An output power of 150 W is delivered at 80–90 A.

To understand the behaviour of each cell during stack operation, the various cell voltages were collected at the bipolar plate terminals. These are shown in Figure 3

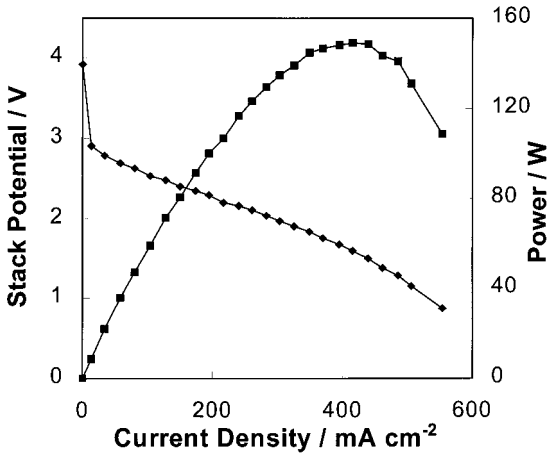

Fig. 2. Galvanostatic polarization data for the five-cell air-feed DMFC stack at 110 °C.

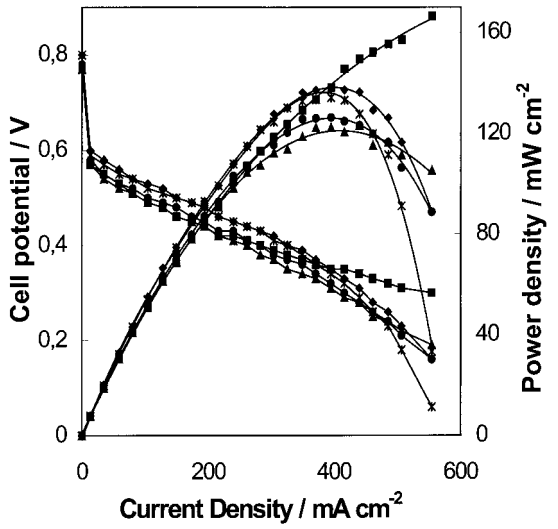

Fig. 3. Galvanostatic polarization data and power densities at 110 °C for the various cells along the DMFC stack section from the reactant inlet. Key: (■) cell 1, (◆) cell 2, (▲), cell 3, (●) cell 4 and (✶) cell 5.

against current density together with their respective power density outputs. The open circuit voltages are similar, ranging between 0.77 and 0.8 V. There are only slight differences in the electrochemical behaviour of the various cells in the activation-controlled region at low current densities. The difference in cell voltages does not exceed 40 mV up to 200 mA cm^{-2}. The last cell (no. 5) along the stack section from the inlet, performed better in the activation-controlled region with respect to the first. The slope of the I/V curves at intermediate current densities is very similar for the various cells, showing that there are no significant differences in terms of internal resistance for the various assemblies. This was confirmed by measurement of the ohmic drop on each cell using the current-interruption method. The first cell in the stack with respect to the reactant inlet does not show a limiting current at high current densities and its corresponding power density increases progressively without reaching a maximum in the current range investigated. The power output for the first cell is about 170 mW cm^{-2} at 550 mA cm^{-2}. The other cells show power densities of between 120 and 140 mW cm^{-2}. They are affected by mass-transport limitations to different extents, the last cell (cell no. 5) showing the most significant constraints. In all the experiments carried out, cell voltage at high current densities decreases almost regularly from the first (cell no. 1) to the last (cell no. 5). Since there was no change in temperature profile at various cells, such differences are ascribed to a nonhomogeneous distribution of reactants along the stack section. Although the reactants enter from one side, they are distributed in parallel to each cell along the stack section and subjected to the same pressure imposed on both anodic and cathodic compartments through backpressure regulators at the reactant outlets. At this time, the source of such mass-transfer losses is not individualized. Investigation and modification in the DMFC stack design are currently being pursued at De Nora Fuel Cells and Sodeteg and they should provide an improved design for the second-term objective which involves the development of a 1 kW stack. One other aspect related to the same phenomenon relies on the different behaviour at low current densities between cell 1 and 5 (Figure 4). The larger cell voltage losses observed in this region for cell 1 are attributed to a larger methanol concentration gradient at the anode–membrane interface with a consequent increase of methanol cross-over through the electrolyte. If, on the one hand, the fuel mass transport rate is significantly larger with respect to the reaction rate, methanol accumulates at the interface and permeates through the electrolyte under the diffusion driving force. On the other hand, this accumulation of methanol at the interface plays a favourable role at high current densities, diminishing cell discharge due to rapid fuel consumption.

To evaluate the scale-up of the system from a 5 cm^2 graphite single cell to a 150 W stainless-steel stack, the polarization characteristics of cells 1 and 5 of the stack are compared in Figure 4 with those recorded in the small prototype under identical conditions. The graphite

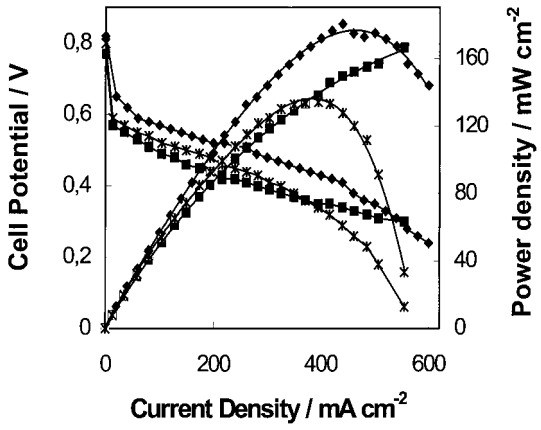

Fig. 4. Comparison of galvanostatic polarization data and power densities for cells 1 (■) and 5 (✱) in the stack and the 5 cm^2 graphite single cell (◆) at 110 °C.

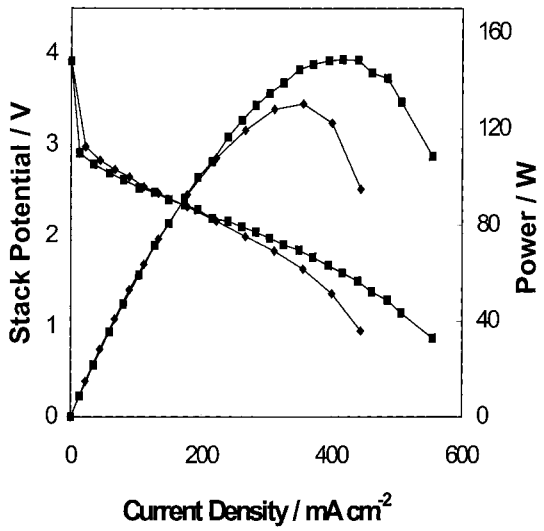

Fig. 5. Comparison of galvanostatic polarization data and power densities for the five-cell DMFC stack at 110 °C during the first stage of the experiments (■) and after one month of discontinuous operation (◆).

cell performs slightly better in the activation-controlled region. Since the electrodes employed in the two devices are identical, this aspect could be ascribed to improved use of the electrode surface area in the graphite cell; further investigations are in progress. The most significant difference between stack cells and the graphite cell is due to the internal resistance value (0.25 Ω cm^2 against 0.11 Ω cm^2). Accordingly, the maximum power density for the graphite cell is significantly higher at intermediate current densities. At 400 mA cm^{-2}, the power loss in the stack cell vs. the small graphite cell due to the different ohmic behaviour only, is about 25 mW cm^{-2}. Thus, another aspect that needs to be addressed for further stack development is the ohmic drop. At first glance, the main source of increased ohmic loss in the stack appears to be due to contact resistance between each electrode backing and metallic foam. The foam is designed so as to have a sufficient degree of porosity, at the same time achieving a good compromise between electrical contact and mass transport. Further developments are currently underway, aiming at decreasing all contact resistances in the system.

One significant aspect concerns stack start-up under practical conditions (e.g., in an electric vehicle). Preliminary experiments carried out on the five-cell stack on self-start-up at room temperature and ambient pressure with 1 M methanol impregnated anodes gave an instant power of 13 W. This is probably not sufficient, at present, to drive all the auxiliaries needed to bring the 150 W stack up to suitable conditions in a very short time. However, all stack characteristics are optimised for operation at high temperature and suitable pressure; more investigation on self start-up is therefore needed.

After one month of discontinuous stack operation under various operating conditions (start-up in the morning and shut-down during the night) no significant change in stack performance was observed at low and intermediate current densities up to 250 mA cm^{-2}, whereas, a slight decrease in limiting current was registered. Figure 5 shows the polarization curves recorded in the first stage of stack operation and after one month's operation. The internal resistance did not change significantly, showing that no passivation process is currently affecting the metal components. Chemical analysis of outlet aqueous solutions from both anode and cathode compartments revealed no loss of metal ions and no apparent change was observed in the stainless steel plates after one month operation. The observed increase of mass transport limitations may be attributed to some modification occurring in the reactant flow within the stack.

4. Conclusions

A five-cell 150 W air-feed stack was demonstrated within the framework of the Nemecel Project. Catalysts, electrodes, stack housing and test bench were developed by the various partners. An average power density approaching 150 mW cm^{-2} was achieved at 110 °C in the presence of 1 M methanol and air feed at 3 atm. The main limitations observed in the DMFC stack related to the homogeneous distribution of reactants and internal resistance. Accordingly, specific advances are needed for the stack components, especially the system housing and reactant flow fields. Subsequent developments will concern the application of high temperature and highly conductive cross-over resilient membranes as an alternative to Nafion®.

Acknowledgements

Collaboration in this project by Solvay (Belgium), University of Poitiers (France), CNRS–LMOPS (Lyon-France) and PSA (France) is greatly appreciated. The Nemecel Project is being developed with the financial support of the European Commission, Directorate General XII, Programme Joule III.

References

1. K. Kordesch and G. Simader, 'Fuel Cells and their Applications' (VCH, Weinheim, 1996).
2. A. Hamnett, *Phil. Trans. R. Soc. Lond.* **A354** (1996) 1653.
3. M.P. Hogarth and G.A. Hards, *Platinum Metal Rev.* **40** (1996) 150.
4. C. Lamy and J-M. Léger, *in* O. Savadogo and P.R. Roberge (Eds), Proc. 2nd International Symp. on 'New Materials for Fuel Cells and Modern Battery Systems', Montréal, Canada (1997), pp. 477–487.
5. A.K. Shukla, P.A. Christensen, A. Hamnett and M.P. Hogarth, *J. Power Sources* **55** (1995) 87.
6. L. Liu, C. Pu, R. Viswanathan, Q. Fan, R. Liu and E.S. Smotkin, *Electrochim. Acta* **43** (1998) 3657.
7. X. Ren, M.S. Wilson and S. Gottesfeld, *J. Electrochem. Soc.* **143** (1996) L12.
8. A.S. Aricò, P. Creti, P.L. Antonucci and V. Antonucci, *Electrochem. Solid State Lett.* **1** (1998) 4.
9. S.R. Narayanan, W.Chun, T.I. Valdez, B. Jeffries-Nakamura, H. Frank, S. Surampudi, G. Halpert, J. Kosek, C. Cropley, A.B. LaConti, M. Smart, Q. Wang, G. Surya Prakash and G.A. Olah, Program and Abstracts, Fuel Cell Seminar (1996), pp. 525–8.
10. M. Baldauf and W. Preidel, *J. Power Sources* **84** (1999) 161.
11. S. Wasmus and A. Kuver, *J. Electroanal. Chem.* **461** (1999) 14.
12. A.S. Aricò, A.K. Shukla, K.M. el-Khatib, P. Cretì and V. Antonucci, *J. Appl. Electrochem.* **29** (1999) 671.
13. A. Hamnett and B.J. Kennedy, *Electrochim. Acta* **33** (1988) 1613.
14. K. Scott, W.M. Taama, P. Argyropoulos and K. Sundmacher, *J. Power Sources* **83** (1999) 204.
15. S. Cleghorn, X. Ren, S. Thomas and S. Gottesfeld, 'Book of Extended Abstracts', 1997 ISE-ECS Joint Symposium, Paris, Sept. (1997), Abstract 182, pp. 218–219.
16. A.S. Aricò, P. Creti, H. Kim, R. Mantegna, N. Giordano and V. Antonucci, *J. Electrochem. Soc.* **143** (1996) 3950.
17. S. C. Thomas, X. Ren and S. Gottesfeld, *in* S. Gottesfeld and T.F. Fuller (Eds), 'Proton Conducting Fuel Cells in Proton Conducting Membrane Fuel Cells' (Second International Symposium), Proc. **98–27**, (Electrochemical Society, Pennington, NJ, 1999), pp. 267–272.
18. T.J. Schmidt, H.A. Gasteiger and R.J. Behm, *Electrochem. Commun.* **1** (1998) 1.
19. M. Gotz and H. Wendt, *Electrochim. Acta* **43** (1998) 3637.
20. K. Lasch, L. Jorissen and J. Garche, *in* C. Lamy and H. Wendt (Eds), Proceedings of the Workshop 'Electrocatalysis in Indirect and Direct Methanol PEM Fuel Cells', 12–14 Sept. (1999), Portoroz, Slovenia, p. 104.
21. H. Kim and A. Wieckowski, *in* O. Savadogo (Ed), Third International Symposium. on 'New Materials for Fuel Cells and Modern Battery Systems', Montrèal, Canada (1999), pp. 125–126.
22. R.M. Moore, S. Gottesfeld and P. Zelenay, *in* S. Gottesfeld and T.F. Fulles (Eds), Proceedings, ref. [17], **98–27,** (1999), pp. 365–379.
23. B.D. McNicol, D.A.J. Rand and K.R. Williams, *J. Power Sources* **83**, (1999) 15.
24. M. Watanabe and S. Motoo, *J. Electroanal. Chem.* **60** (1975) 275.
25. P.S. Kaurenan and E. Skou, *J. Electroanal. Chem.* **408** (1996) 189.
26. P.L. Antonucci, A.S. Aricò, P. Cretì, E. Ramunni and V. Antonucci, *Solid State Ionics* **125** (1999) 431.